ORIGINAL ARTICLE

Adsorption of stable and labile emerging pollutants on activated carbon: degradation and mass transfer kinetic study

Eva Díaz[1] · Laura García[1] · Salvador Ordóñez[1]

Abstract

The design of adsorption processes for pharmaceuticals removal depends not only on the adsorption equilibrium but also on the mass transfer and adsorbate stability, being a problem still not solved the case of degradation products. By selecting different stable (amoxicillin, ciprofloxacin, carbamazepine and ibuprofen) and labile micropollutants (omeprazole) as case studies emerging pollutants, we have quantitatively analysed these effects on activated carbon. For stable compounds, the experimental data were fitted to equilibrium models to obtain information about the different adsorption mechanism depending on the characteristics of the molecules. Mass transfer effects were analysed for all the adsorbates, observing the control of intraparticle pore diffusion mechanism, since the effective pore diffusion coefficient is in the range from 10^{-8} to 10^{-10} cm^2 h^{-1}. As far as omeprazole is concerned, a kinetic model is proposed for predicting its degradation, identifying the reversibility of several degradation steps. The overall adsorption of OMP and derivates is calculated, observing the pore diffusion is considered as the rate-limiting step. For the first time, a combined model considering the chemical degradation and the adsorption of the degradation products is proposed and experimentally validated. This represents an important step in the modelling of processes leading to the purification of water from this type of pollutant.

Keywords Micropollutants · Adsorption equilibrium · Mass transfer coefficients · Reactive adsorbates · Activated carbons

Introduction

The release of different kinds of micropollutants (as drugs and drug metabolites) to wastewater is arising as a major environmental issue for the forthcoming years. Most of these micropollutants (also called emerging pollutants, EP) are hydrophilic and refractory to biological degradation. Thus, they are not efficiently removed in conventional wastewater treatment facilities, being finally released to natural water bodies (Mailler et al., 2015). Once these pollutants are in the environment, different transformations occur, sometimes producing products that can differ in their environmental behaviour and ecotoxicological profile. Among the available treatment technologies, adsorption on activated carbon stands out due to its advantages as low cost, high efficiency,

simplicity in the layout, lower maintenance and versatility for different compounds (Aboua et al., 2015; Martín et al., 2018; Cheng et al., 2021; Fallah et al., 2021).

The performance of activated carbons to remove EP from water samples has been addressed, including thermodynamic (feasibility, capacities and adsorption equilibrium considering Langmuir and Freundlich approaches), and, to a minor extent, kinetic studies. The few reported kinetic models do not consider variables directly related to the adsorption process (mass transfer, diffusion and adsorption on the active site) and only describe the behaviour (Moreno-Pérez et al., 2021). At this point, adsorption on a microporous solid, such as the activated carbon, is typically controlled by the intraparticle diffusion step, whereas film diffusion and adsorption steps are usually faster (Schwaab et al., 2017; Inglezakis et al., 2020). With this background, it is striking that a limited number of works deal with the diffusion models for the estimation of liquid–solid mass transfer coefficients on adsorption models (Fulazzaky et al., 2013; Tian et al., 2016; Inglezakis et al., 2020; Amarasinghe et al., 2020).

Regarding adsorbates, some authors observed that adsorbate characteristics highly influence the adsorption behaviour

✉ Salvador Ordóñez
sordonez@uniovi.es

1   Catalysis, Reactors and Control Research Group (CRC),
    Department of Chemical and Environmental Engineering,
    University of Oviedo, Julián Clavería S/N, 33006 Oviedo,
    Spain

of several adsorbates on the adsorbent (Patiño et al., 2015). However, several pharmaceuticals and pesticides are reactive and, hence, may undergo different chemical, physical and biological processes modifying the adsorption behaviour (Mijangos et al., 2019). At this point, the stability of amoxicillin is largely studied, observing degradation after an induction period (Palma et al. 2016; Samara et al., 2017). Likewise, omeprazole degradation is observed to begin without an induction period, although slow in absence of light (DellaGreca et al., 2006; Nevado et al., 2013). Despite the existence of these unstable compounds, and although many works deal with the adsorption of a variety of stable emerging pollutants onto microporous adsorbents, to the best of our knowledge, any of them is focused on the adsorption of labile pollutants, as well as its derived species.

In this context, the present research provides a systematic study on the adsorption of different emerging pollutants (amoxicillin, ciprofloxacin, carbamazepine, ibuprofen and omeprazole) on activated carbon. In that way, experimental data of different stable compounds were fitted to the adsorption isotherms to obtain information about the adsorption mechanism. Likewise, the influence of mass transfer in the adsorption was studied by the calculation of mass transfer and diffusion coefficients. As a novelty, the adsorption of a compound that decomposes over time (omeprazole) is studied in a differentiated way. We propose for this last case adsorption models considering both the reaction and the intermediates adsorption.

Experimental section

Materials

Powdered activated carbon employed in the experiments was supplied by Norit (NORIT SAE SUPER). According to the supplier, the adsorbent has an average particle size (D_{50}) of 20 µm, an apparent density of 375 kg m^{-3}, a total surface area of 1050 m^{2}g^{-1} and a pore volume of 0.95 cm^{3}g^{-1}, with a main contribution of mesopores (0.81 cm^{3}g^{-1}) (Kampouraki et al., 2019), as measured from the Brunauer–Emmett–Teller (BET) experiments.

Carbamazepine and omeprazole were obtained from ACROS ORGANICS (VWR, USA). Ibuprofen, ciprofloxacin and amoxicillin (potency: $\geq$ 900 µg per mg) were acquired from Sigma-Aldrich (USA). All chemicals have a purity $\geq$ 98%. The molecular structures of each adsorbate, as well as the physicochemical properties, are listed in Table 1. More concretely, pKa was obtained from the DrugBank database, taking the experimental value with the exception of AMX, for which is not available, so predicted on is included. Molecular weight has been obtained either from this database, or from Molinspiration, together with volume

and topological polar surface area (TPSA). The application, available online, allows you to draw the molecule and calculate molecular properties from it. Finally, water solubility and log K_{OW} were obtained from Chemaxon.

The HPCL grade solvents used are: acetonitrile ($\geq$ 99.9%); di-sodium hydrogen phosphate anhydrous; sodium phosphate monobasic monohydrate ($\geq$ 98%) and phosphoric acid (85%).

Determination of pollutant stability

Different 50 mL distilled water solutions of amoxicillin, carbamazepine, ciprofloxacin, ibuprofen and omeprazole, at the highest concentration which avoids pharmaceuticals saturation at 25 °C (100, 75, 50, 20 and 75 mg L^{-1}, respectively), were kept in a water bath (Memmert) with agitation, at 25 °C, in absence of light, for a minimum of 24 h to ensure equilibrium. Samples (1.5 mL) were collected and analysed at regular intervals of time by high-performance liquid chromatography (HPLC).

Adsorption experiments

Batch adsorption experiments were performed in 100 mL glass bottles shaken in a water bath 100 opm (oscillations per minute). Preliminary tests were conducted at 25 °C to determine the equilibrium time and to fix the optimum adsorbent loading, varying the activated carbon concentration from 0.05 to 0.5 g L^{-1}. From these experiments, experimentation time was selected in order to ensure the equilibrium: omeprazole, ciprofloxacin and amoxicillin, 24 h, whereas ibuprofen and carbamazepine, 8 and 7 h, respectively.

Adsorption isotherms were conducted at 25, 35 and 45 °C for each pharmaceutical. The amount of activated carbon established in the preliminary experiments (5 mg) was mixed with 100 mL glass bottle with solutions of the micropollutants in concentrations between 5 and 100 mgL^{-1}, depending on its solubility in water and its limit of detention in the HPLC. Blank experiments were also carried out under the same conditions to consider the losses of adsorbate by volatilization and by degradation of the unstable compounds. Once equilibrium was reached, supernatants were filtered using syringe nylon filters prior its analysis. All the experiments were done by duplicate, as well as the analysis. Supernatants analysis provides the equilibrium liquid phase composition, whereas solid-phase composition was calculated using a mass balance.

Analytical detection

The concentrations of the emerging pollutants were analysed by HPLC in an Agilent 1200 model equipped with an UV–Vis detector and a 150 mm Zorbax Extend-C18 column.

Table 1 Main physicochemical properties of the emerging pollutants used in this work

Compound	Molecular structure	pKa[1]	Molecular weight[1,2]	logK_{OW}[3]	Water solubility[3] (g L^{-1})	Volume[2] (A^3)	TPSA[2] (A^2)
Amoxicillin (AMX)		3.2	365	−1.35	0.02	306.89	132.96
Ibuprofen (IBP)		5.3	206	3.46	0.06	211.19	37.3
Carbamazepine (CBZ)		15.9	236	2.84	0.04	215.08	48.03
Ciprofloxacin (CIP)		6.09	331	−0.7	1.61	285.46	74.57
Omeprazole (OMP)		9.29	345	2.41	0.11	302.81	77.11
Omeprazole degradation products							
B		–	329	4	–	295.26	–
D		–	315	–	–	277.73	–
C	n.a	–	284	–	–	–	–

[1]Obtained from DrugBank (https://go.drugbank.com/drugs)

[2]Obtained from Molinspiration (www.molinspiration.com/cgi-bin/properties)

[3]Obtained from Chemaxon. (http://www.chemaxon.com)

Amoxicillin was detected in a wavelength of 230 nm using ultrapure water (Milli-Q) (solvent A) and acetonitrile (solvent B) as mobile phases. Elution of amoxicillin started with 5% solvent B for 10 min linear gradient to 53% solvent B with a flow rate of 1 mL min^{-1}. The volume of injection was 40 μL and the operation temperature was 30 °C.

Carbamazepine, ciprofloxacin and omeprazole were analysed in wavelengths of 210, 280 and 280 nm, respectively, using an isocratic solution of mobile phase consisting of 700:300 phosphate buffer: acetonitrile with the pH adjusted to 7 with phosphoric acid. The buffer was prepared by mixing 839 mg of di-sodium hydrogen phosphate anhydrous and 136 mg of sodium phosphate monobasic monohydrate in 1 L of Milli-Q water. Then, the solution was filtered with 0.2 μm nylon membrane filters prior being used as mobile phase. The volume of injection, operational flow rate and temperature were 20 μL, 2 mL min^{-1} and 25 °C, respectively.

Ibuprofen was detected in a wavelength of 214 nm using a mixture of Milli-Q water adjusted to pH 2.5 with phosphoric acid and acetonitrile (400:600) as mobile phase. 10 μL of the micropollutant was injected

in an isocratic flow rate of 1.7 mL min^{-1} and an operation temperature of 20 °C.

Omeprazole degradation products were identified by LC–MS/MS experiments, carried out on an Agilent 1260 Infinity LC system coupled to a Triple Quad™ 6500 MS. Electrospray ionization was performed in the positive mode (ESI+) with a source temperature of 300 °C. Parameters used to produce fragment ions were a declustering potential (DP) of 40 V, a collision cell exit potential (CXP) of 6 V and a collision energy (CE) of 45 V. Chromatographic separation was achieved analogous to that previously described.

Results and discussion

Stability of pharmaceuticals

Figure 1 shows that amoxicillin (AMX), ibuprofen (IBP), carbamazepine (CBZ) and ciprofloxacin (CIP) were stable compounds in water for, at least, a day scale. After one day, AMX also starts a slight degradation process; however, since the adsorption equilibrium time is reached before (24 h), this compound can be treated as a stable one. In agreement, even 14 days were reported in the literature as degradation time for AMX at 25 °C (Palma et al. 2016). Furthermore, the European Commission service (Marianini et al., 2017) confirmed the CBZ and IBP stability after 10 weeks of an isochronous stability study.

A different situation is observed for OMP, which concentration decreases constantly with time until reaching at 55 h a quarter of its initial concentration (Fig. 1). In agreement, Nevado et al. (2013) observed, for a 40 mg L^{-1} water solution of OMP, in absence of light at 20 °C, total disappearance after 50 h.
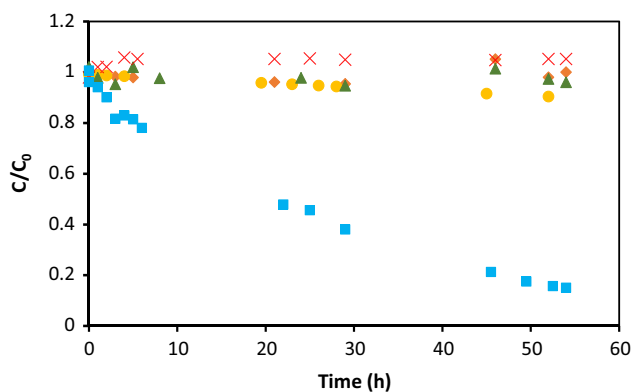
Fig. 1 Stability experiments at 25 °C for amoxicillin (circle), carbamazepin (triangle), ciprofloxacin (diamond), ibuprofen (red) and omeprazole (square). Initial concentrations: 100, 75, 50, 20 and 75 mg L^{-1} for amoxicillin, carbamazepine, ciprofloxacin, ibuprofen and omeprazole, respectively

Therefore, in the following sections, the stable compounds will be treated separately of the labile one, omeprazole, since for the latter a study of the species in which it decomposes will be made, as well as its ability to interact with the activated carbon.

Stable compounds

Adsorption isotherms

The influence of adsorbent concentration on the adsorption of the considered pollutants is plotted in Fig. S1. The amount of adsorbate retained per unit of adsorbent decreased when the adsorbent mass is increased, following the order: CBZ > CIP > AMX > IBP. To maximize the adsorbate loading and the removal efficiency, the activated carbon concentration was set to 0.05 g L^{-1} for all compounds.

Experimental equilibrium data at 25 °C for carbamazepine (CBZ), ciprofloxacin (CIP), ibuprofen (IBP) and amoxicillin (AMX) are presented in Fig. S2. The amount of adsorbate retained, at same temperature and equilibrium concentration, follows the order: CIP > CBZ > AMX > IBP. Both CIP and AMX reach the maximum capacity of adsorption (about 400 mg/g), although in the case of CIP with a lower equilibrium concentration. Usually, adsorbate size and weight control the accessibility into the adsorbent pores; however, in this case, AMX exhibits the largest size and a very worthy value of adsorption capacity. Contrary, IBP, with the smallest size, presents the lowest adsorption capacity. This fact suggests that the morphology of the adsorbate is not the limiting factor, but other forces could play a key role in the interaction (Wu et al., 2020). Attending to the electrostatic interactions, Kampouraki et al. (2019) measured for the activated carbon of this work an acidic to basic groups ratio very low (0.08), with presence of two kinds of oxygen functional groups on carbon's surface (lactones and phenols), and a point of zero charge (pzc) of 9.9. Therefore, operating at pH (7), the adsorbent surface is positively charged due to the protonation of the lactones and phenols groups. According to the adsorbates dissociation constant, as shown in Table 1, CBZ is not dissociated at operating conditions. Thus, electrostatic attraction cannot explain its adsorption capacity. Contrary, CIP, AMX and IBP are partially deprotonated, acquiring anionic character. Therefore, an adsorbate/adsorbent electrostatic attraction can explain the high adsorption capacities obtained for AMX and CIP. Another adsorption mechanism, based on π–π stacking interaction, justifies the CBZ elevated adsorption capacity. CBZ molecule, with three aromatic rings, would have a special affinity towards activated carbon, surface lactones playing also a fundamental role. This trend could be deduced from its high octanol–water partition coefficient (2.84), which is known to increment the potential retention by soil and

sediments, as shown in Table 1. However, the largest log Kow value of IBP could not justify its modest adsorption capacity.

Hydrogen bonding is also a very common mechanism in the adsorption of organic compounds (Valencia et al., 2018). Although hydrogen bonding is possible for all the emerging pollutants, this interaction is more limited in the case of IBP—in comparison with CIP, CBZ and AMX—since it has only $a = O$ hydrogen acceptor and a –OH hydrogen donor groups.

To get further insights about the IBP adsorption mechanisms, Fig. S2 also includes the isotherms models fitting curves. Experimental data were fitted to two-parameter adsorption isotherms: Freundlich, Langmuir, Temkin, Harkin–Jura, Fowler–Guggenheim, Hill-Deboer and Jovanovic. The equations of these isotherms, as well as the assumptions, are summarized in Table S1. Likewise, Table 2 includes the obtained parameters, associated with surface characteristics, affinity of the adsorbent and adsorption capacity of the adsorbent. The goodness of the fitting of the different models provides interesting insights about the adsorption mechanisms, highlighting the different character of the adsorbate–adsorbent interactions.

As given in Fig. S1 and Table 2, Langmuir isotherm is the most appropriate for describing AMX adsorption, also showing the largest monolayer adsorption. Likewise, the value of q_m for CBZ is slightly higher than reported by Li et al. (2011) on activated carbon, 287 mg/g.

The K_F values of Freundlich isotherm, largest for CBZ and CIP, are in agreement with the experimental results. In the same way, a very similar value of K_F was reported to adsorption of CBZ on powdered activated carbon (163 $(mg\ g^{-1})(L\ mg^{-1})^{1/n}$) (Delgado et al., 2019). Concerning the exponent, n, values in the range 2–10 represent good adsorption features, so all the adsorbates are in this group. Similarly, Yu et al. (2008) obtained n values between 1.14 and 3.3 for the adsorption of aromatic compounds when activated carbons were used as adsorbents, and Sharifpour et al. (2020) in the adsorption of CIP on activated carbon coated with multiwalled carbon nanotubes obtained $K_F = 372$ (mg $g^{-1})(L\ mg^{-1})^{1/n}$.

With the exception of AMX, best determination coefficients were obtained from Freundlich than Langmuir isotherm (Table 2), suggesting adsorption on heterogeneous surfaces as could be expected given the surface chemistry of the activated carbon. However, there is still possibility for improvement in the fitting coefficients. Therefore, other less common adsorption models (Temkin, Harkin–Jura, Fowler–Guggenheim, Hill-Deboer and Jovanovic) have been also studied.

Temkin model predictions are quite close to experimental data, being remarkable the high value of K_T obtained for CBZ, in agreement with the K_L value of Langmuir

isotherm; confirming in this way the equilibrium of the process. Analogously, the low K_T for AMX would highlight the irreversibility of the process. Concerning b constants are in all cases positive, suggesting the unfavourable thermodynamic adsorption between the adsorbates and activated carbon (Tian et al., 2016), especially in the case of IBP. Hill-Deboer fitting is really poor in the case of AMX; thus, the hypothesis of mobile adsorption among the adsorption sites and the lateral interaction can be discarded. For the rest of adsorbates, although with better fitting coefficients, this model also presents a worse fit than previous models. The fitting of Fowler–Guggenheim model allows directly discard this model for AMX. For the other adsorbates, with $R^2 > 0.9$, their positive ω values are congruent with attractive forces among the adsorbed molecules, especially for CBZ and CIP. This fact is in agreement with the bad fit of CBZ and CIP to Langmuir model, which assumes no interaction among adsorbed molecules. Harkin–Jura model can be, once again, discarded for AMX, whereas quite good fitting was obtained for CIP, suggesting multilayer adsorption.

Concerning the Jovanovic model, the values of q_{max} obtained in the fitting procedure were found to be slightly lower than experimental data. The K_J constant was in all cases negative and close to 0, being these values very similar to other authors (Díaz de Tuesta et al. 2020). The negative value of the constant is due to isotherm equation expression respect to the inlet exponential content. As given in Table 2, this model fits with a great accuracy the IBP experimental data; thus, adsorption of IBP can be better explained by approximation of monolayer localized adsorption with surface binding vibrations of an adsorbed species.

Mass transfer effects on the adsorption

The pollutant adsorption is governed by the consecutive steps: (1) diffusion across the liquid film surrounding the sorbent particles (film diffusion); (2) intraparticle diffusion from surface through the pores to internal activate sites (pore diffusion) and (3) adsorption on the adsorbent active sites (adsorption) (Amarasinghe et al., 2020). For the adsorption, the main diffusion resistance is likely to be film or intraparticle diffusion.

To assess these effects, the Weber–Morris equation, derived from Fick's law for adsorbate diffuse in spherical adsorbent particles at a short adsorption time, is propose for predicting the rate-controlling step (Sekulic et al., 2019). This model can be expressed as follows (Sahmoune et al., 2011; Tian et al., 2016), Eq. 3:

$$q_t = k_{id}t^{0.5} + C \tag{3}$$

where k_{id} is the intraparticle diffusion rate constant (mg g^{-1} $h^{-0.5}$) and C (mg g^{-1}) is the intercept linked to the

Table 2 Amoxicillin, ibuprofen, carbamazepine and ciprofloxacin adsorption parameters

Langmuir

Compounds	K_L (L mg^{-1})	q_m (mg g^{-1})	R^2
AMX	0.077	463	0.992
CBZ	0.33	361	0.809
IBP	2.84	65	0.937
CIP	1.93	320	0.887

Freundlich

Compounds	K_F ((mg g^{-1})(L mg^{-1})$^{1/n}$)	n	R^2
AMX	109	3.26	0.947
CBZ	172	5.33	0.981
IBP	46	4.90	0.974
CIP	188	5.40	0.963

Temkin

Compounds	b (kJ mol^{-1})	K_T (L mg^{-1})	R^2
AMX	0.027	0.99	0.988
CBZ	0.064	133.20	0.982
IBP	0.211	47.75	0.968
CIP	0.051	43.32	0.950

Hill-Deboer

Compounds	K_1 (L mg^{-1})	K_2 (kJ mol^{-1})	R^2
AMX	0.0057	14.73	0.282
CBZ	0.044	23.48	0.749
IBP	0.00026	39.82	0.919
CIP	0.776	4.57	0.892

Fowler–Guggenheim

Compounds	K_{FG} (L mg^{-1})	ω (kJ mol^{-1})	R^2
AMX	0.01	-2.38	0.283
CBZ	9.26	5.25	0.971
IBP	2.34	0.93	0.946
CIP	15.03	7.62	0.921

Harkin–Jura

Compounds	A	B	R^2
AMX	141,482	5.1	0.221
CBZ	93,153	2.4	0.937
IBP	7747	3.6	0.845
CIP	71,424	2.0	0.987

Jovanovic

| Compounds	q_{max} (mg g^{-1})	K_J (L mg^{-1})	R^2
AMX	231	-0.008	0.953
CBZ	190	-0.013	0.777
IBP	42	-0.082	0.993
CIP	196	-0.023	0.983

apparent thickness of the film boundary layer (Sahmoune et al., 2011).

From Fig. 2, it is observed that in the case of CBZ a straight line intercepts the origin, suggesting an adsorption process solely governed by intraparticle diffusion (Zhu et al., 2016). However, two different zones are observed of the other compounds, where the straight lines do not intercept the origin, indicating that intraparticle diffusion is involved, but not being the only rate-limiting step. This behaviour was already reported for adsorption of cationic dyes and emerging pharmaceuticals (Sahmoune et al., 2011; Tian et al., 2016; Sekulic et al., 2019). At a first insight, from the difference between CBZ and the rest of pollutants, it can be inferred that deprotonated forms of the compounds would increase the thickness of the film layer. Figure 2 and Table 3 show that the first stage, linked to boundary layer

effect, presents higher slope than the second one, related to intraparticular diffusion and hence $k_{id1} > k_{id2}$; thus, at a first insight the film diffusion will not be rate limiting.

Comparison of k_{id} values remarks the influence of the micropollutant molecular sizes, since the lowest k_{id} values correspond to CIP and AMX, molecules with the greatest molecular weights (331 and 365 g/mol, respectively). In this way, Sekulic et al. (2019) studied the adsorption of several EP onto phosphorous-doped microporous carbonaceous materials obtaining for CBZ and IBP both k_{id} and C values lower than the observed in this study (14 mg g^{-1} h$^{-0.5}$, 4.4 mg g^{-1}; 15 mg g^{-1} h$^{-0.5}$ and 4.7 mg g^{-1} for CBZ and IBP, respectively). These differences can be justified both by the lower operation temperature (20 °C versus 25 °C) and lower initial concentration in the case of CBZ (20 mg L^{-1} versus 75 mg L^{-1}).

Fig. 2 Intraparticle diffusion model of amoxicillin (circle), carbamazepine (triangle), ciprofloxacin (diamond) and ibuprofen (square) adsorption onto activated carbon. Experiments were conducted at 25 °C, and initial concentrations of AMX, CBZ, CIP and IBP are 100, 75, 50 and 20 mgL-1, respectively
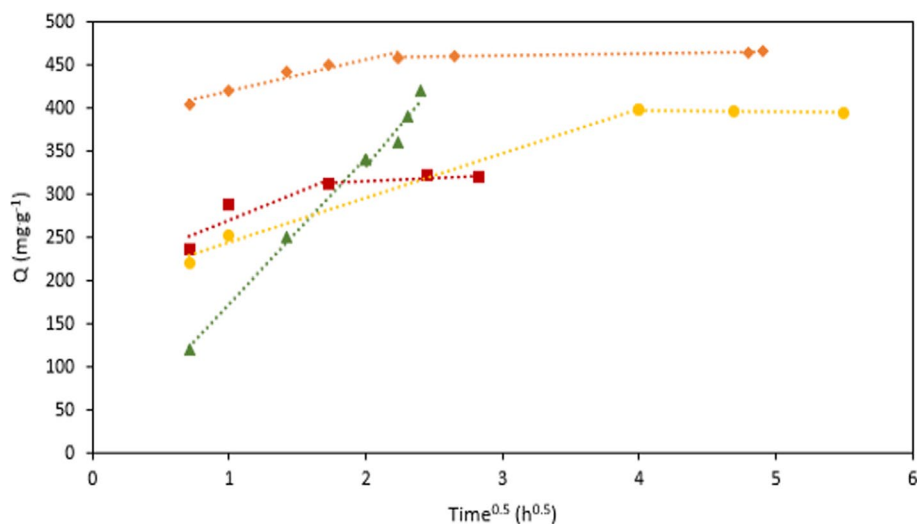
Table 3 Coefficients for the different mass transfer models of amoxicillin, carbamazepine, ciprofloxacin and ibuprofen adsorption onto activated carbon

Pharmaceutical		AMX	CBZ	CIP	IBP	OMP	B	D	C
Intraparticle diffusion model	k_{id1} (mg g^{-1} h$^{-0.5}$)	51.72	–	36.56	65.04	118			
	k_{id2} (mg g^{-1} h$^{-0.5}$)	1.45	166	2.33	10.17	47			
	C_1 (mg g^{-1})	192	–	383	205	526			
	C_2 (mg g^{-1})	392	0	454	267	664			
	R_1^2	0.991	–	0.937	0.797	0.999			
	R_2^2	1	0.983	0.974	0.616	0.994			
Overall mass transfer model	k_L (m h^{-1})	3.24×10^{-3}	2.65×10^{-3}	7.34×10^{-3}	8.18×10^{-3}	4.31×10^{-3}	4.76×10^{-3}	2.11×10^{-3}	1.29×10^{-3}
	C_{eq} (µmol L^{-1})	220	238.4	82.4	34.5	56	0.65	19	21
	R^2	0.980	0.931	0.993	0.995	0.813			
Pore diffusion model	D_i (cm^2 h^{-1})	3.36×10^{-8}	6.04×10^{-8}	6.85×10^{-8}	5.07×10^{-8}	1.70×10^{-8}			
	R^2	0.996	0.946	0.588	0.876	0.764			

Furthermore, it is also observed from CBZ data that the intraparticle diffusion rate increases with increasing initial EP concentration in solution, since higher initial concentration leads to higher concentration gradient, which will eventually cause faster diffusion and quicker adsorption.

In order to combine both the film diffusion and diffusion in the particle together, the mass transfer model was applied, where the overall mass transfer coefficient (k_L, m h^{-1}) can be obtained from Eq. 4:

$$\frac{dC}{dt} = -k_L S(C - C_{eq}) \qquad (2)$$

where S is the surface area of the adsorbent per unit volume of the particle-free solution (m^{-1}) and C_{eq} is the solute concentration in the solution in equilibrium with the adsorbent at time t.

Table 3 shows a decreasing order of mass transfer coefficients ($k_{L\_IBP} > k_{L\_CIP} > k_{L\_AMX} > k_{L\_CBZ}$) with the adsorbate equilibrium concentrations ($C_{eqIBP} < C_{eqCIP} < C_{eqAMX} < C_{eqCBZ}$), which matches with the decreasing adsorbate initial concentrations (Fig. S3).

Likewise, the effective pore diffusion coefficient (D_i, cm^2 h^{-1}) was calculated from Eq. 5 (Tian et al., 2016):

$$-log\left[1 - \left(\frac{q}{q_e} \right)^2 \right] = \frac{4\pi^2 D_i t}{2.3 d_p^2} \qquad (3)$$

where q (mg g^{-1}) and qe (mg g^{-1}) are the adsorbate concentration in the adsorbent at time t and at equilibrium and d_p (cm) is the mean adsorbent diameter. As given in Table 3, all adsorbates present similar D_i, being only remarkable that AMX, with the highest volume (307 A^3), exhibits the lowest diffusivity and CIP, with the highest dipole moment (9.98 D), has the highest diffusivity. On the other hand, values between 2.41 10^{-11} cm^2 h^{-1} and 1.9 10^{-3} cm^2 h^{-1} (Frölich et al., 2018; Deng et al., 2019; Moreno-Pérez et al., 2021) where reported for EP adsorption on carbon nanotubes or biochars. It is convenient to outline that, in agreement with Micherlsen et al. (1975), mass transfer processes for all the adsorbates are controlled by intraparticle pore diffusion mechanism, since the D_i is in the range from 10^{-8} to 10^{-10} cm^2 h^{-1}.

The key role of the adsorbate in the mass transfer is shown in Fig. S4, where the k_L (Fig. S4a) and the k_{id2} coefficient (Fig. S4b) (characteristic of the intraparticular diffusion) are plotted versus the molecular weight of the adsorbates. It can be observed a continuous decreasing trend in the overall mass transfer coefficient and the intraparticular diffusion coefficient with the molecular size for IBP, CIP and AMX. The discordant role of CBZ can be justified attending to the pKa of the molecule, being the

only non-deprotonated molecule in the operation conditions. In fact, from the Temkin adsorption isotherms, it was observed a very high equilibrium constant for CBZ, compatible with a chemisorption process, which could be responsible of the different behaviour.

Adsorption of reactive adsorbates: Omeprazol

Firstly, the adsorbent amount was optimized for OMP adsorption, selecting, analogous to stable compounds, a concentration of activated carbon of 0.05 gL^{-1}.

Omeprazole degradation products and kinetic modelling

Figure 1 shows the instability of OMP in a water media after 55 h. A comprehensive analyses of the reaction products showed that the main reaction products of the OMP ($C_{17}H_{19}N_3O_3S$) degradation are omeprazole sulphide (B) ($C_{17}H_{19}N_3O_2S$), 4-hydroxy omeprazole sulphide (D) ($C_{16}H_{17}N_3O_2S$) and $C_{14}H_{28}N_4O_2$ (C). The evolution of the concentration these degradation products is shown in Fig. 3a. Quantification details of the species and mass balance details are summarized in Text S1.

Based on the degradation pathway proposed by Schmidt et al. (2014), the concentration of the different species was fitted to several models using MATLAB. The model with the best fitting (based on the degradation pathway proposed in (Fig. 3b) was selected on the basis of regression coefficient $R^2 = 0.991$. Equations of the pseudo-first-order kinetics are detailed in Eq. 6–9.

$$-\frac{dC_{OMP}}{dt} = k_1 C_{OMP} \qquad (4)$$

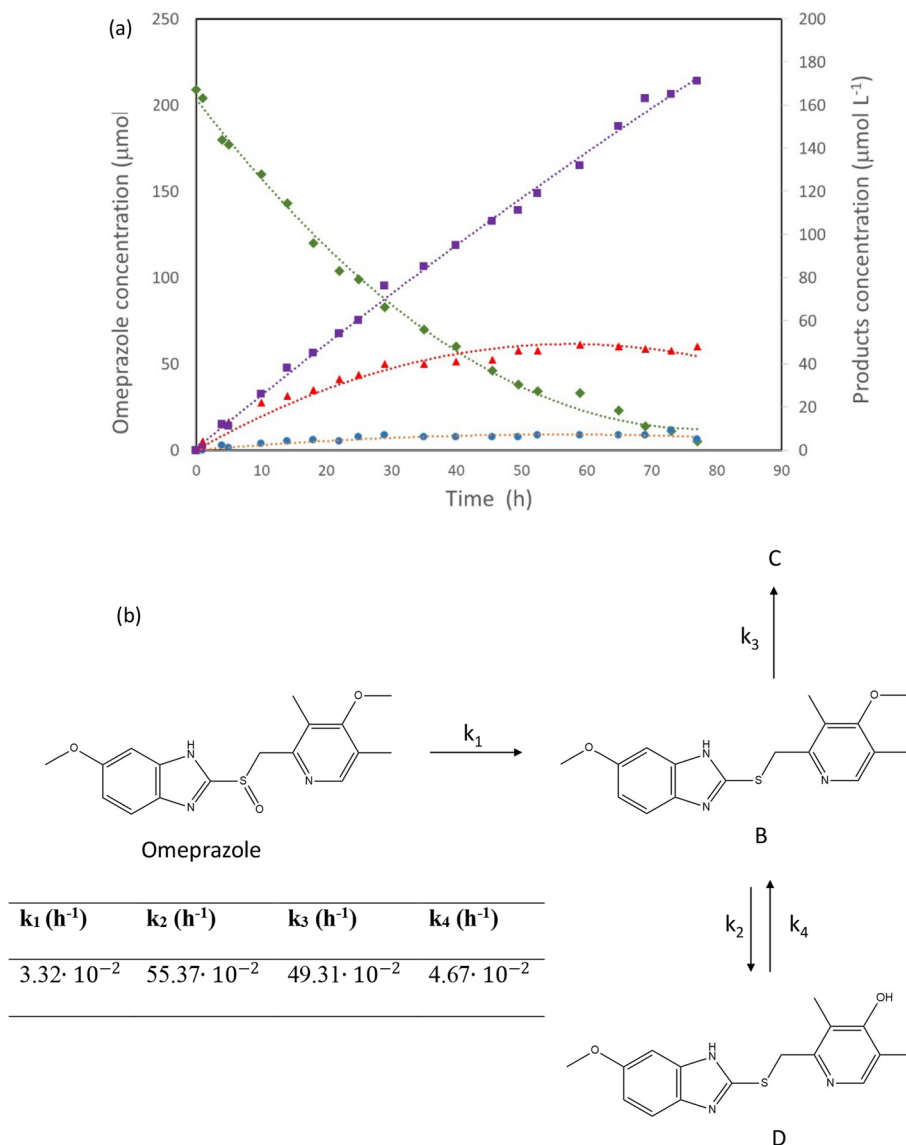$$\frac{dC_B}{dt} = k_1 C_{OMP} - k_3 C_B - k_2 C_B + k_4 C_D \qquad (5)$$

$$\frac{dC_C}{dt} = k_3 C_B \qquad (6)$$

$$\frac{dC_D}{dt} = k_2 C_B - k_4 C_D \qquad (7)$$

where C (µmol L^{-1}) and k (h^{-1}) are the concentration and the degradation rate constant of the studied compound, respectively. The kindness of the fitting is shown in Fig. 3a and kinetic constants in Fig. 3b.

OMP degradation reaction into B is slow in absence of light (DellaGreca et al., 2006; Nevado et al., 2013), yielding to the lowest value of the kinetic constant (k_1 of 3.32 10^{-2} h^{-1}). This OMP decomposition into the sulphide (B) can be explained since sulfoxides are fragmented or reduced via cations and the conversion can occur more easily with

Fig. 3 **a** Omeprazole degradation kinetic model obtained from omeprazole stability experiments at 25 °C and at an initial concentration of 75 mg L^{-1}: (diamond) omeprazole, (circle) (**B**), (square) (**C**), (triangle) (**D**). **b** Omeprazole degradation pathway proposed in this work

k_1 (h^{-1})	k_2 (h^{-1})	k_3 (h^{-1})	k_4 (h^{-1})
$3.32 \cdot 10^{-2}$	$55.37 \cdot 10^{-2}$	$49.31 \cdot 10^{-2}$	$4.67 \cdot 10^{-2}$

heterocyclic compounds (DellaGreca et al., 2006), being also slow at conditions of low acidity as it is the case (pH below 7). In fact, El-Badry et al. (2009), working at 25 °C and pH = 7.5, obtained a kinetic degradation constant of 0.0037 h^{-1}, justified due to the highest OMP stability in alkaline medium.

The intermediate B is decomposed following two parallel routes, yielding D and C, respectively. The first reaction is reversible, although the direct one ($k_2 = 55.37\,10^{-2}$ h^{-1}) is faster than the reverse ($k_4 = 4.67\,10^{-2}$ h^{-1}). This pathway was also proposed by Jadhav et al. (2016), although it is not still reported in any pharmacopeia. Concerning C, this compound is tentatively shown by LC–MS detection, although, to the best of our knowledge, it was never described as degradation product of OMP. At this point, B has a benzimidazole group which shows a high photosensitivity to degradation in solution (2006). Therefore, this molecule could break through the imine bond (C=N) of the benzimidazole group. Then, two fragments of this molecule could join together to form C.
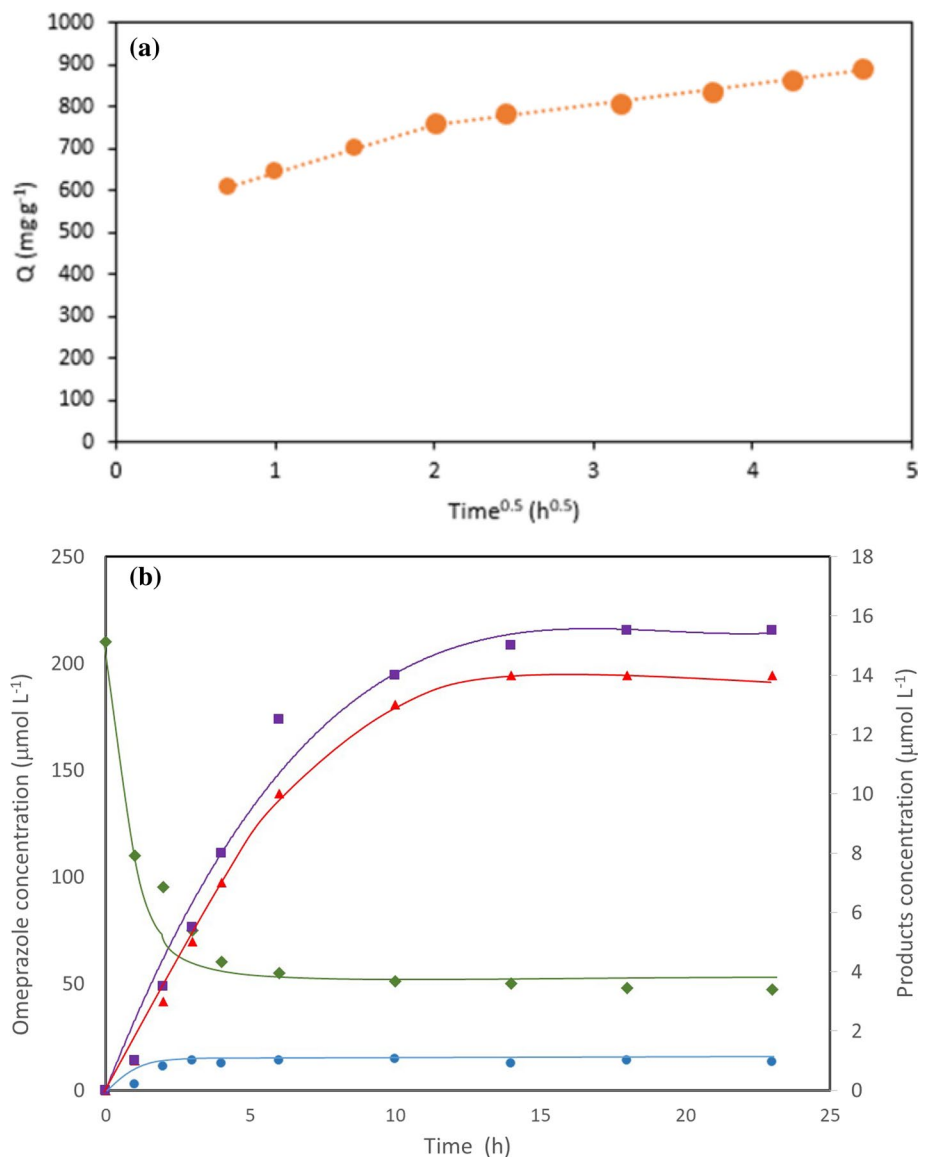
OMP and its degradation products adsorption behaviour

Experimental adsorption capacities of OMP and their degradation products, calculated in basis of the carbon balance (Text S2), are shown in Fig. 4a.

The kinetic data were further fitted to the intraparticle diffusion model, observing two differenced zones. The first is related to the film diffusion and the second one, which with the lower value is the limiting step, to the intraparticular diffusion.

Finally, and similar to the mass transfer analysis of the stable compounds, the intraparticle diffusion coefficient (D_i) was calculated. Its value, $1.70\,10^{-8}$ cm^2 h^{-1}, also

Fig. 4 a Global adsorption capacities among time of omeprazole and its degradation products. **b** External film diffusion model for omeprazole and its degradation products: (diamond) omeprazole, (circle) B, (square) C, (triangle) D

justifies that the pore diffusion is considered as the rate-limiting step (Michelsen et al. 1975).

Overall mass transfer process and modelling

OMP and its degradation products have been independently fit to the overall mass transfer model, in order to get an overall view of the adsorption and degradation of this pollutant. In this model, OMP degradation rate constants from the previously reported model were considered (Fig. 3b), were also considered, whereas equilibrium concentrations and the overall mass transfer coefficients were the fitting parameters. Governing equations are summarized in Eqs. 10–13, whereas modelling results are shown in Fig. 4b, and the resulting coefficients are summarized in Table 3.

$$\frac{dC_{OMP}}{dt} = -k_1 \cdot C_{OMP} - k_{LOMP}S(C_{OMP} - C_{eqOMP}) \tag{10}$$

$$\frac{dC_B}{dt} = k_1 \cdot C_{OMP} - k_2 \cdot C_B - k_3 \cdot C_B + k_4 \cdot C_D - k_{LB}S(C_B - C_{eqB}) \tag{11}$$

$$\frac{dC_D}{dt} = k_2 \cdot C_B - k_4 \cdot C_D - k_{LD}S(C_D - C_{eqD}) \tag{12}$$

$$\frac{dC_C}{dt} = k_3 \cdot C_B - k_{LC}S(C_C - C_{eqC}) \tag{13}$$

The highest mass transfer coefficients were obtained for OMP and OMS (4.31×10^{-3} and 4.76×10^{-3} m h^{-1}, respectively), and this despite the fact that they are the molecules with a higher molecular weight, as shown in

Table 1. Attending to the pKa of both compounds, 9.29 and 9.81 for OMP and B, respectively, both compounds are not dissociated at the operating pH, whereas it could be assumed that C and D are dissociated, hence their different behaviour. Moreover, the high values of log K_{ow} of OMP and B could justify also their easiness in the mass transfer. By contrast, the hydroxyl group of D could suppose a greater hydrophilic character, difficulting in this way the mass transfer.

The kinetic constants of Fig. 3b, as well as the overall mass transfer coefficients of Table 3, were used to predict the evolution with time of OMP and degradation products at different initial concentrations, and results were compared to experimental ones (Fig. S5). As a result, modelled results fit experimental data with an acceptable accuracy.

Conclusion

Adsorption of stable (CIP, AMX, CBZ and IBP) and labile (OMP) pharmaceuticals onto activated carbon has been studied in this article. Specifically, adsorption equilibrium isotherms (for stable compounds), mass transfer and diffusion coefficients have been calculated and an omeprazole degradation pathway has been developed, proposing a kinetic model based on mass transfer coefficients.

From adsorption equilibrium modelling, the adsorption mechanisms of the different EP considered were deduced, pointing out the differences among adsorbates. In the case of AMX, an irreversible and endothermic interaction in monolayer was deduced and without interaction among the adsorbed molecules (Langmuir and Temkin isotherms). From Temkin isotherm, it is observed a reversible adsorption process for CBZ. Moreover, all the adsorbates, excepting AMX, but mainly CIP and CBZ, present interaction among the molecules, as it is observed from Fowler–Guggenheim isotherm. And IBP, as it is deduced from Jovanovic isotherm, can experiment mechanical contacts between the adsorbate and adsorbent.

The kinetic mass transfer limiting step of the adsorption process was analysed for each adsorbate with the Weber–Morris equation, observing that the intraparticle diffusion is the slowest step in all cases. This result was confirmed by the intraparticle diffusion coefficient (D_i), with values around 10^{-8} cm^2 h^{-1}. Furthermore, it was observed a continuous decreasing trend in the overall mass transfer and intraparticular diffusion coefficients with the molecular size for IBP, CIP and AMX, being attributed the discordant role of CBZ to the pKa of the molecule.

Finally, the degradation compounds of OMP at 25 °C for 77 h were identified, fitting the experimental data to a first-order kinetic model. Likewise, the concentrations of OMP and its derivated in presence of activated carbon were fitted to a model based on mass transfer coefficients, confirming also in this way the limiting step of the intraparticle diffusion.

Declarations

References

Aboua KN, Yobouet YA, Yao KB, Goné DL, Trokourey A (2015) Investigation of dye adsorption onto activated carbon from the shells of Macoré fruit. J Environ Manage 156:10–14. https://doi.org/10.1016/j.jenvman.2015.03.006

Amarasinghe P, Amarasinghe K (2020) Determination of mass transfer coefficients for adsorption of Pb and Cd onto coir pith and statistical analysis. J Anal Tech Res 2:137–148. https://doi.org/10.26502/jatri.017

Cheng N, Wang B, Wu P, Lee X, Xing Y, Chen M, Gao B (2021) Adsorption of emerging contaminants from water and wastewater by modified biochar: a review. Environ Poll 273:116448. https://doi.org/10.1016/j.envpol.2021.116448

Delgado N, Capparelli A, Navarro A, Marino D (2019) Pharmaceutical emerging pollutants removal from water using powdered activated carbon: study of kinetics and adsorption equilibrium. J Environ Manage 236:301–308. https://doi.org/10.1016/j.jenvman.2019.01.163

DellaGreca M, Lesce MR, Previtera L, Rubino M, Temussi F, Brigante M (2006) Degradation of lansoprazole and omeprazole in the aquatic environment. Chemosphere 63:1087–1093. https://doi.org/10.1016/j.chemosphere.2005.09.003

Deng Y, Ok YS, Mohan D, Pittman CU, Dou X (2019) Carbamazepine removal from water by carbon dot-modified magnetic carbon nanotubes. Environ Res 169:434–444. https://doi.org/10.1016/j.envres.2018.11.035

Díaz de Tuesta JL, Silva AMT, Faria JL, Gomes HT (2020) Adsorption of Sudan-IV contained in oily wastewater on lipophilic activated

carbons: kinetic and isotherm modelling. Environ Sci Pollut R 27:20770–20785. https://doi.org/10.1007/s11356-020-08473-1

El-Badry M, Taha EI, Alanazi FK, Alsarra IA (2009) Study of omeprazole stability in aqueous solution: influence of cyclodextrins. J Drug Deliv Sci Tech 19:347–351. https://doi.org/10.1016/S1773-2247(09)50072-X

Fallah Z, Zare EN, Ghomi M, Ahmadijokani F, Amini M, Tajbakhsh M, Arjmand M, Sharma G, Ali H, Ahmad A, Makvandi P, Lichtfouse E, Sillanpää M, Varma RS (2021) Toxicity and remediation of pharmaceutical and pesticides using metal oxides and carbon nanomaterials. Chemosphere 275:130055. https://doi.org/10.1016/j.chemosphere.2021.130055

Frölich AC, Ocampo-Pérez R, Diaz-Blancas V, Salau NPG, Dotto GL (2018) Three-dimensional mass transfer modeling of ibuprofen adsorption on activated carbon prepared by sonication. Chem Eng J 341:65–74. https://doi.org/10.1016/j.cej.2018.02.020

Fulazzaky MA, Khamidun MH, Omar R (2013) Understanding of mass transfer resistance for the adsorption of solute onto porous material from the modified mass transfer factor models. Chem Eng J 228:1023–1029. https://doi.org/10.1016/j.cej.2013.05.100

Inglezakis VJ, Balsamo M, Montagnaro F (2020) Liquid-Solid mass transfer in adsorption systems-An overlooked resistance? Ind Eng Chem Res 59:22007–22016. https://doi.org/10.1021/acs.iecr.0c05032

Jadhav SB, Kumar CK, Bandichhor KR, Bhosale PN (2016) Development of RP UPLC-TOF/MS, stability indicating method for omeprazole and its related substances by applying two level factorial design; and identification and synthesis of non-pharmacopoeial impurities. J Pharmaceut Biomed 118:370–379. https://doi.org/10.1016/j.jpba.2015.10.005

Kampouraki ZC, Giannakoudakis DA, Triantafyllidis KS, Deliyanni EA (2019) Catalytic oxidative desulfurization of a 4,6-DMDBT containing model fuel by metal-free activated carbons: the key role of surface chemistry. Green Chem 21:6685–6698. https://doi.org/10.1039/c9gc03234g

Li X, Hai FI, Nghiem LD (2011) Simultaneous activated carbon adsorption within a membrane bioreactor for an enhanced micropollutant removal. Bioresource Technol 102:5319–5324. https://doi.org/10.1016/j.biortech.2010.11.070

Mailler R, Gasperi J, Coquet Y, Deshayes S, Zedek S, Gren-Olivé C, Cartiser N, Eudes V, Bressy A, Gaupos E, Moilleron R, Chebbo G, Rocher V (2015) Study of a large scale powdered activated carbon pilot: removals of a wide range of emerging and priority micropollutants from wastewater treatment plant effluents. Water Res 72:315–330. https://doi.org/10.1016/j.watres.2014.10.047

Marianini G, Tavazzi S, Comero S, Buttiglieri G, Paracchini B, Skejo H, Alcande Sanz L, Gawlik BM (2017) Short-term isochronous stability study of contaminants of emerging concern in environmental water samples. JCR Technical Reports. European Commission. doi: https://doi.org/10.2760/488206.

Martin J, Orta MM, Medina-Carrasco S, Santos JL, Aparicio I, Alonso E (2018) Removal of priority and emerging pollutants from aqueous media by adsorption onto synthetic organo-functionalized high-charge swelling micas. Environ Res 164:488–494. https://doi.org/10.1016/j.envres.2018.03.037

Michelsen DL, Gideon JA, Griffith GP, Pace JE, Kutat H L (1975) Removal of soluble mercury from waste water by complexing techniques. Virginia Water Resources Research Center 74

Mijangos L, Urain O, Ruiz-Rubio L, Ziarrusta H, Olivares M, Zuloaga O, Prieto A, Etxebarria N (2019) Short-term stability assessment for the analysis of emerging contaminants in seawater. Environ Sci Pollut Res Int 26:23861–23872. https://doi.org/10.1007/s11356-019-05172-4

Moreno-Pérez J, Pauletto PS, Cunha AM, Bonilla-Petriciolet A, Salau NPG, Dotto GL (2021) Three-dimensional mass transport modeling of pharmaceuticals adsorption inside ZnAl/biochar composite. Colloid Surface A 164:126170. https://doi.org/10.1016/j.colsurfa.2021.126170

Nevado JJB, Peñalvo GC, Dorado RMR, Robledo VR (2013) Study of controlled degradation processes and electrophoretic behaviour of omeprazole and its main degradation products using diode-array and ESI-IT-MS detection. Anal Meth 5:3299–3306. https://doi.org/10.1039/C3AY40460A

Palma E, Ellison L, Meza E, Griko Y (2016) Calorimetric evaluation of amoxicillin stability in aqueous solutions. Mathews J Pharm Sci 2:008

Patiño Y, Díaz E, Ordóñez S (2015) Performance of different carbonaceous materials for emerging pollutants adsorption. Chemosphere 119:S124–S130. https://doi.org/10.1016/j.chemosphere.2014.05.025

Sahmoune MN, Ouazene N (2011) Mass-transfer processes in the adsorption of cationic dye by sawdust. Environ Prog Sustain 31:597–603. https://doi.org/10.1002/ep.10594

Samara E, Moriarty TF, Decosterd LA, Richards RG, Gautier E, Wahl P (2017) Antibiotic stability over six weeks in aqueous solution at body temperature with and without heat treatment that mimics the curing of bone cement. Bone Joint J 6:296–306. https://doi.org/10.1302/2046-3758.65.BJR-2017-0276.R1

Schmidt AH, Stanic M (2014) Rapid UHPLC method development for omeprazole analysis in a quality-by design framework and transfer to HPLC using chromatographic modelling. Lc Gc N AM 32:126–148

Schwaab M, Steffani E, Barbosa-Coutinho E, Júnior JBS (2017) Critical analysis of adsorption/diffusion modelling as a function of time square root. Chem Eng Sci 173:179–186. https://doi.org/10.1016/j.ces.2017.07.037

Sekulic MT, Boskovic N, Slavkovic A, Garunovic J, Kolakovic S, Pap S (2019) Surface functionalised adsorbent for emerging pharmaceutical removal: adsorption performance and mechanisms. Process Saf Environ 125:50–63. https://doi.org/10.1016/j.psep.2019.03.007r

Sharifpour N, Moghaddam FM, Mardani G, Malakootian M (2020) Evaluation of the activated carbon coated with multiwalled carbon nanotubes in the removal of ciprofloxacin from aqueous solutions. Applied Water Sci 10:140. https://doi.org/10.1007/s13201-020-01229-9

Tian J, Guan J, Gao H, Wen Y, Ren Z (2016) The adsorption and mass-transfer process of cationic red X-GRL dye on natural zeolite. Water Sci Tech-W Sup 73:2119–2131. https://doi.org/10.2166/wst.2016.055

Valenia D, García-Cruz I, Ramírez-Verduzco LF, Aburto J (2018) Adsorption of biomass-derived products on MoO_3: hydrogen bonding interactions under the spotlight. ACS Omega 3:14165–14172. https://doi.org/10.1021/acsomega.8b02497

Wu C, Klemes MJ, Trang B, Dichtel WR, Helbling DE (2020) Exploring the factors that influence the adsorption of anionic PFAS on conventional and emerging adsorbents in aquatic matrices. Water Res 182:115950. https://doi.org/10.1016/j.watres.2020.115950

Yu Z, Peldszus S, Huck PM (2008) Adsorption characteristics of selected pharmaceuticals and an endocrine disrupting compound-Naproxen, carbamazepine and nonylphenol-on activated carbon. Water Res 42:2873–2882. https://doi.org/10.1016/j.watres.2008.02.020

Zhu Q, Moggridge GD, D'Agostino C (2016) Adsorption of pyridine from aqueous solutions by polymeric adsorbents MN 200 and MN 500. Part 2: kinetics and diffusion analysis. Chem Eng J 306:1223–1233. https://doi.org/10.1016/j.cej.2016.07.087